



In vitro selection of macrocyclic peptide inhibitors containing cyclic $\gamma^{2,4}$ -amino acids targeting the SARS-CoV-2 main protease

In the format provided by the
authors and unedited

Supplementary Information for:

In vitro selection of macrocyclic peptide inhibitors containing cyclic $\gamma^{2,4}$ -amino acids targeting the SARS-CoV-2 main protease

Takashi Miura¹, Tika R. Malla², C. David Owen^{3,4}, Anthony Tumber², Lennart Brewitz², Michael A. McDonough², Eidarus Salah², Naohiro Terasaka¹, Takayuki Katoh¹, Petra Lukacik^{3,4}, Claire Strain-Damerell^{3,4}, Halina Mikolajek^{3,4}, Martin A. Walsh^{3,4}, Akane Kawamura^{2,5}, Christopher J. Schofield², and Hiroaki Suga^{1*}

¹Department of Chemistry, Graduate School of Science, The University of Tokyo, 7-3-1 Hongo, Bunkyo-ku, Tokyo 113-0033, Japan

²Department of Chemistry and the Ineos Oxford Institute for Antimicrobial Research, Chemistry Research Laboratory, University of Oxford, 12 Mansfield Road, OX1 3TA, Oxford, United Kingdom

³Diamond Light Source, Harwell Science & Innovation Campus, Didcot, Oxfordshire OX11 0DE, United Kingdom

⁴Research Complex at Harwell, Harwell Science & Innovation Campus, Didcot OX11 0FA, United Kingdom

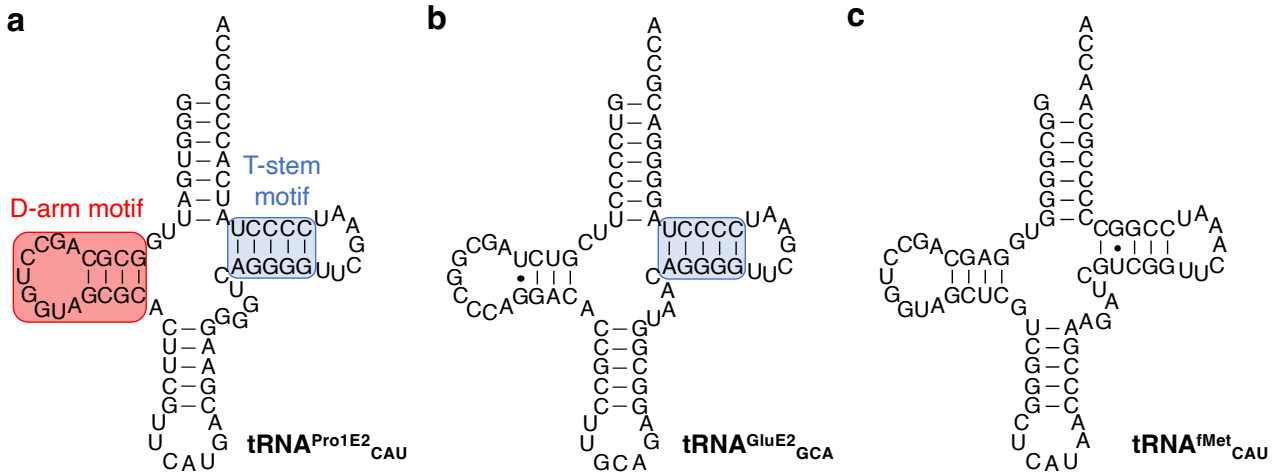
⁵Chemistry – School of Natural and Environmental Sciences, Newcastle University, Newcastle upon Tyne, NE1 7RU, United Kingdom.

*To whom correspondence should be addressed.

E-mail: hsuga@chem.s.u-tokyo.ac.jp (H.S.)

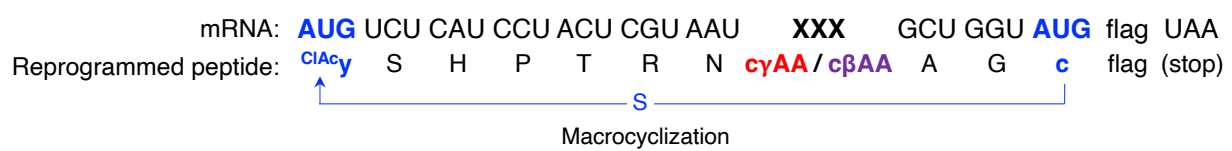
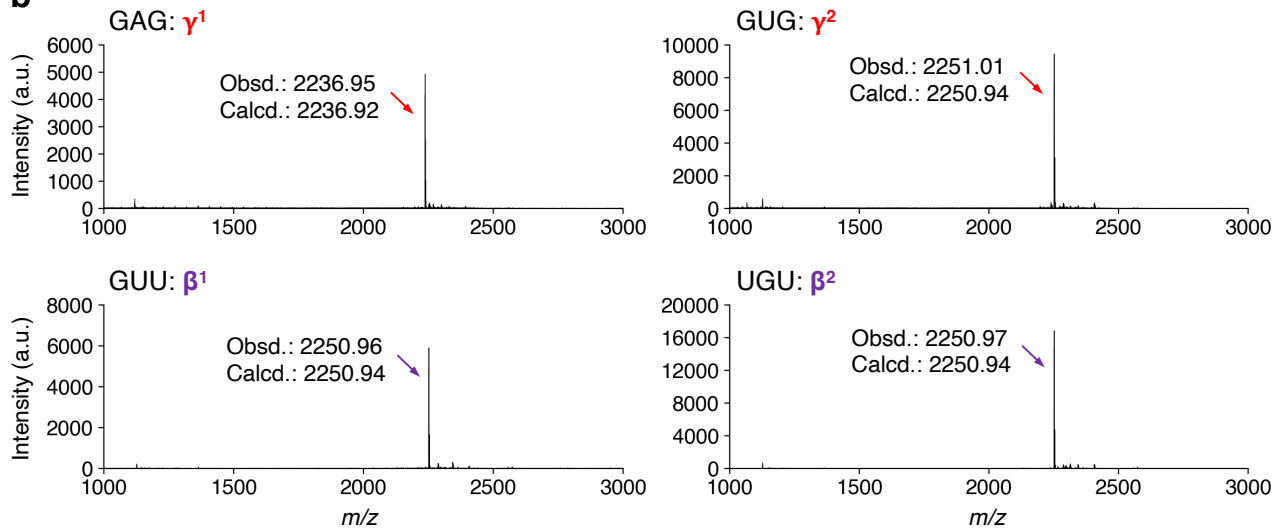
Table of Contents

Title	Page
Supplementary Fig. 1: Secondary structures of tRNAs used for incorporation of c γ AAs, c β AAs, and D-amino acids.	3
Supplementary Fig. 2: Ribosomal synthesis of model macrocyclic peptides containing c γ AA or c β AA.	4
Supplementary Fig. 3: Purities and identities of peptides synthesized by SPPS.	5
Supplementary Fig. 4: Chemical structures of selected peptides by RaPID including the most potent variant GM4H3Q.	7
Supplementary Fig. 5: Binding kinetics of macrocyclic peptides against M ^{pro} .	9
Supplementary Fig. 6: Serum stability assay of macrocyclic peptides.	10

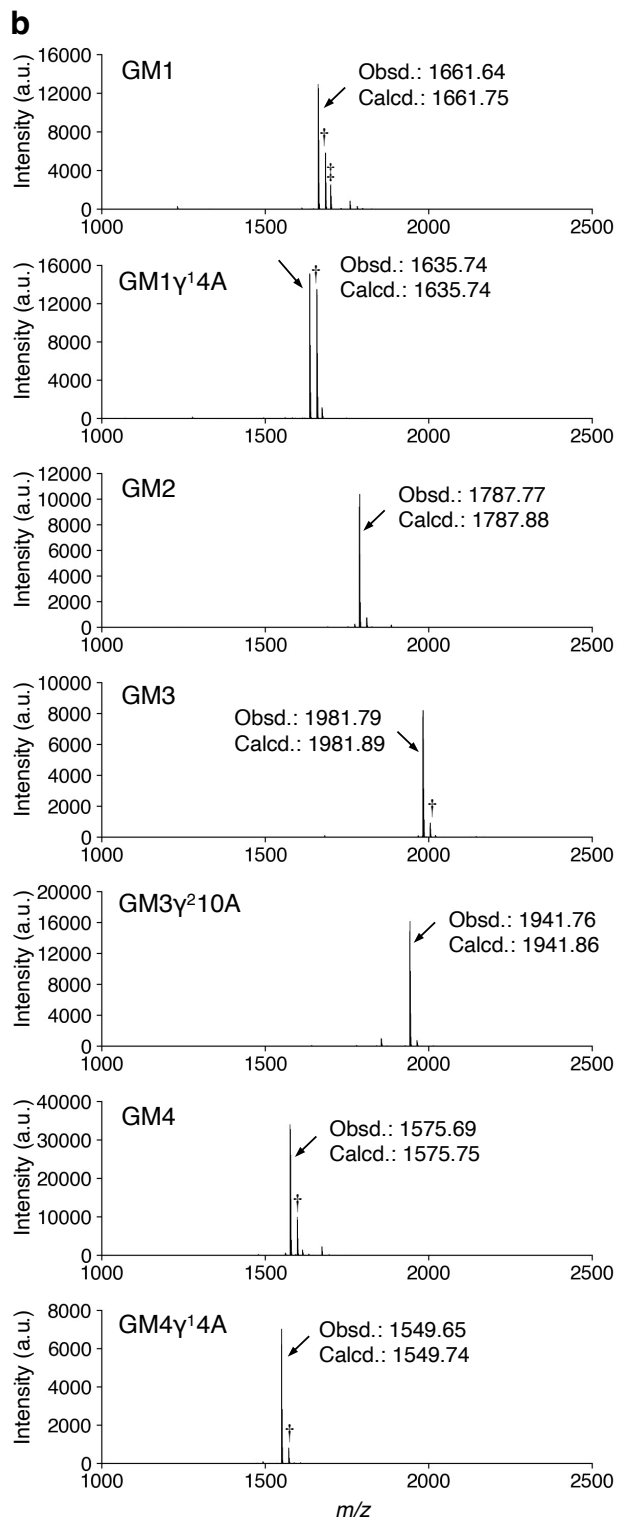
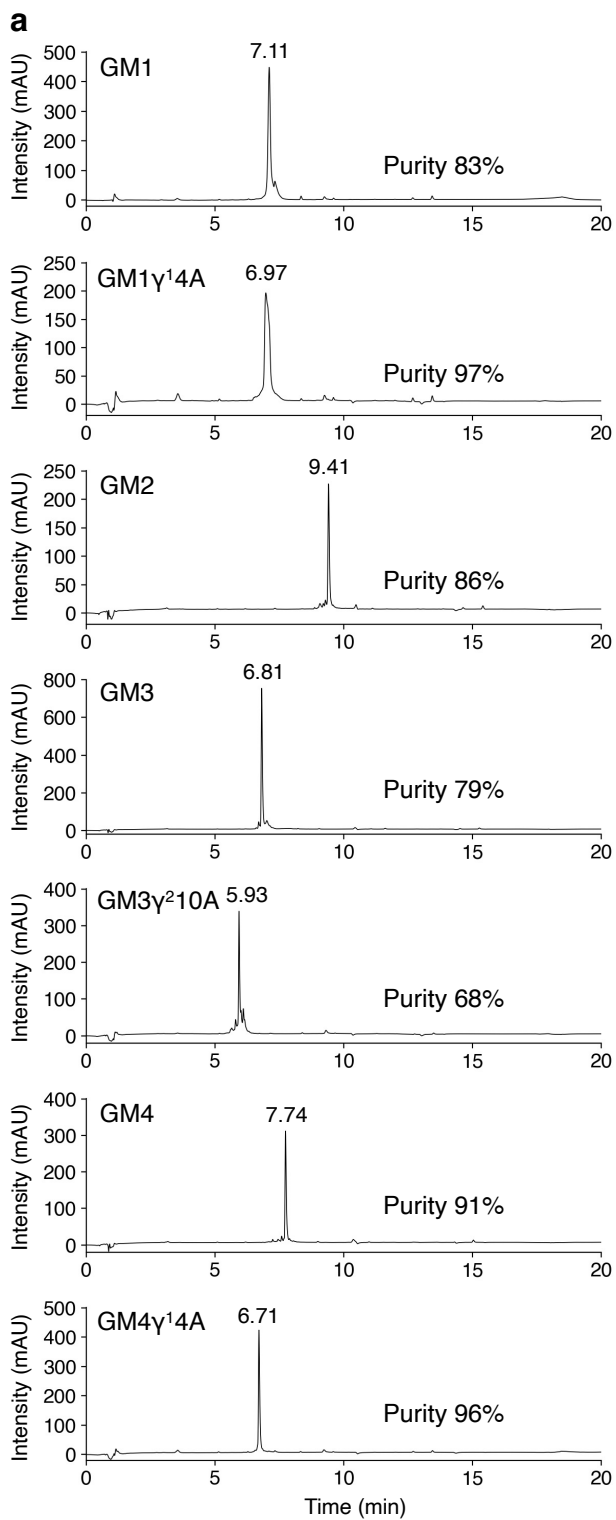


Supplementary Fig. 1: Secondary structures of tRNAs used for incorporation of c γ AAs, c β AAs, and D-amino acids.

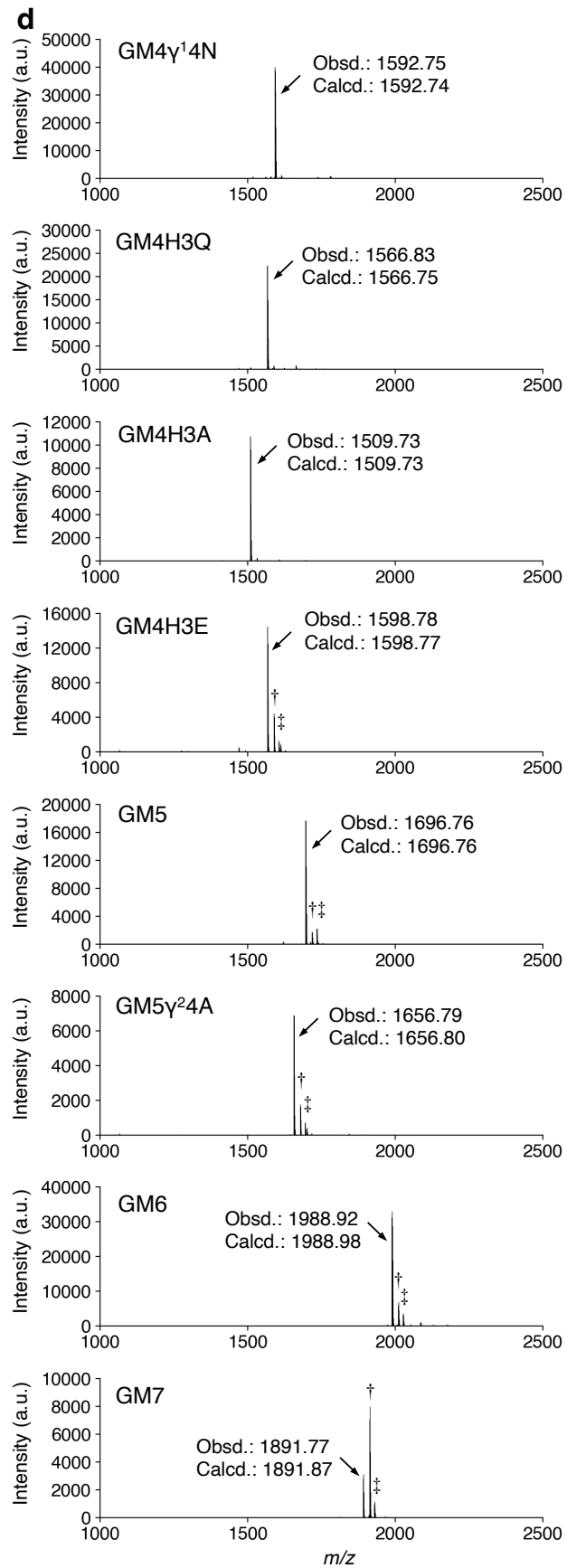
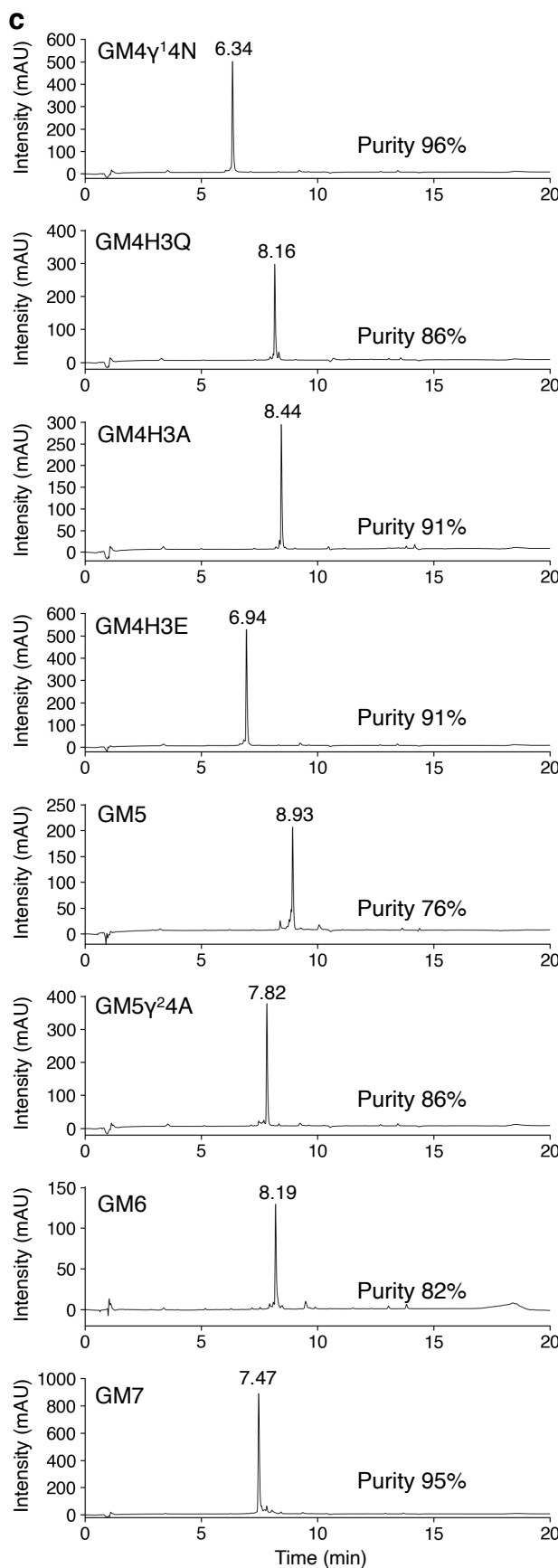
a, tRNA^{Pro1E2}_{CAU} used for decoding AUG codons. For decoding other codons, the sequence of anticodon loop was changed accordingly (see Supplementary Table 3 for the sequences). The D-arm motif for EF-P binding consists of a 9-nt D-loop closed by a stable 4-bp stem (highlighted in red). The T-stem motif for EF-Tu binding is highlighted in blue. **b**, tRNA^{GluE2}_{GCA} used for decoding UGC codons. The T-stem motif for EF-Tu binding highlighted in blue is identical to that of tRNA^{Pro1E2}. **c**, tRNA^{fMet}_{CAU} used for incorporation of ^{ClAc} γ at the initiator AUG codon.

a**b**

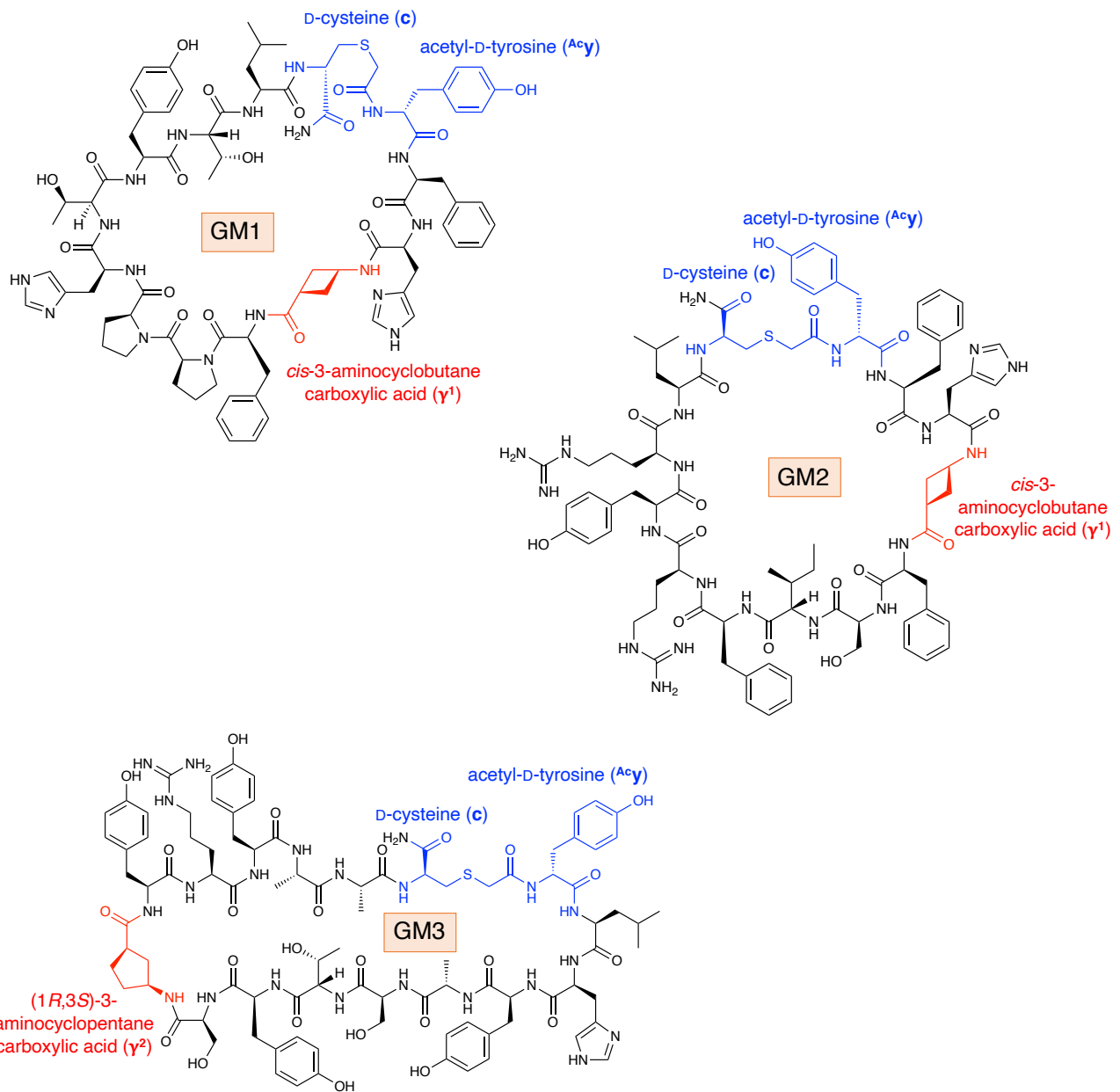
Supplementary Fig. 2: Ribosomal synthesis of model macrocyclic peptides containing c γ AA or c β AA. **a**, Sequence of template mRNA for a model peptide. XXX indicates the codon used for incorporation of c γ AA or c β AA. **b**, MALDI-TOF mass spectra of model peptides. Codons used for incorporation of c γ AA or c β AA are indicated. Calcd. and Obsd. indicate calculated and observed [M+H]⁺ values, respectively.



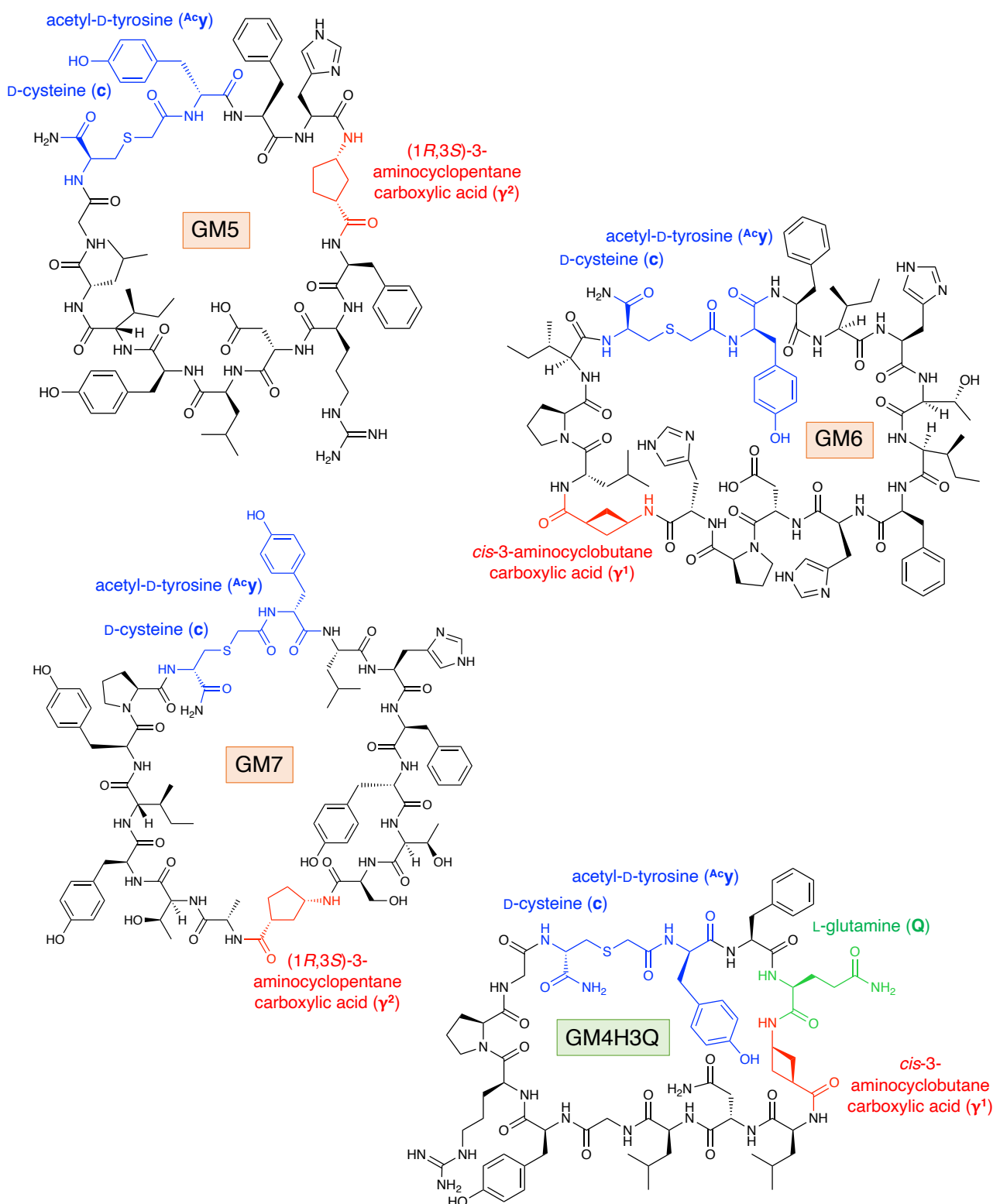
Supplementary Fig. 3: Purities and identities of peptides synthesized by SPPS. **a,c**, UV ($\lambda = 280$ nm) chromatograms of peptides by UPLC. Purity was determined by calculating the ratio of peak area of desired peptide relative to the combined areas of all peaks present. **b,d**, MALDI-TOF mass spectra of peptides. Calcd. and Obsd. indicate calculated and observed $[M+H]^+$ values, respectively. † and ‡ indicate sodium and potassium ion adducts, respectively.



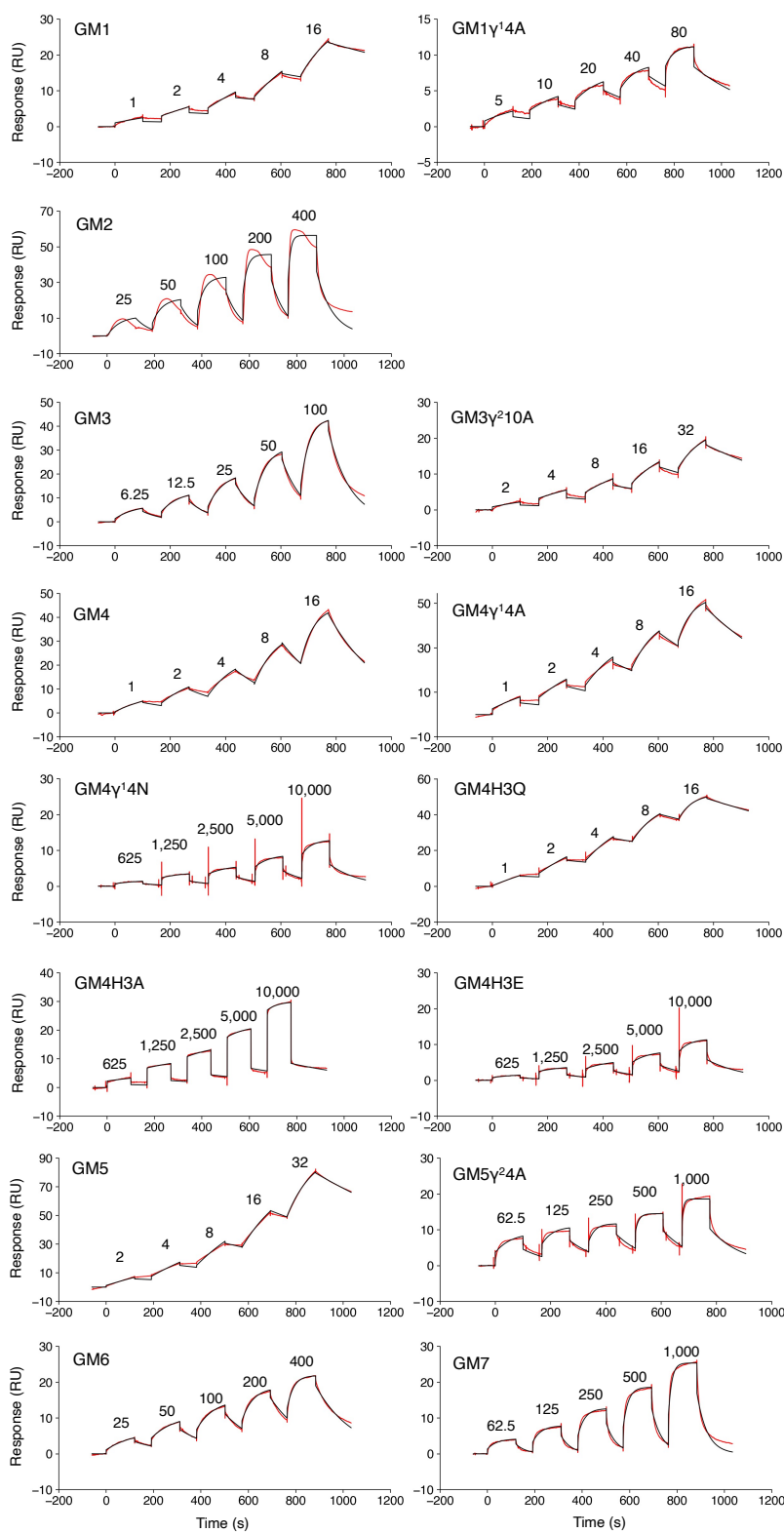
Supplementary Fig. 3, continued.



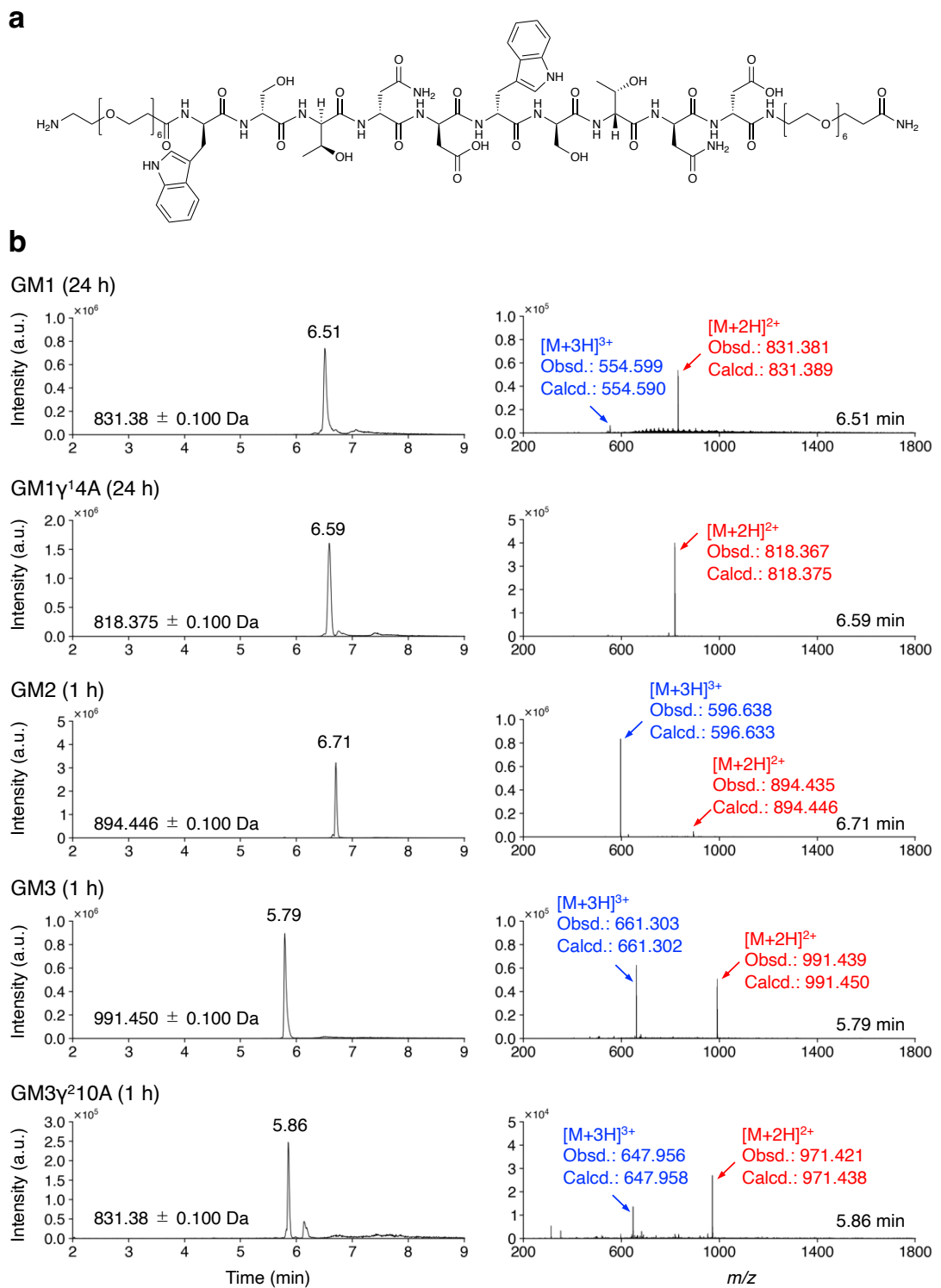
Supplementary Fig. 4: Chemical structures of selected peptides by RaPID including the most potent variant GM4H3Q. See Fig. 3b for GM4.



Supplementary Fig. 4, continued.



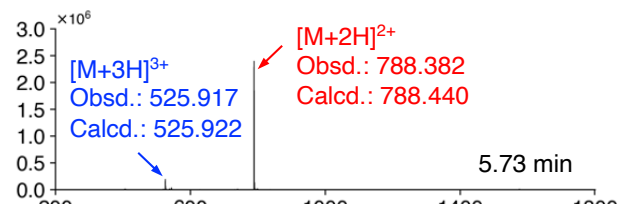
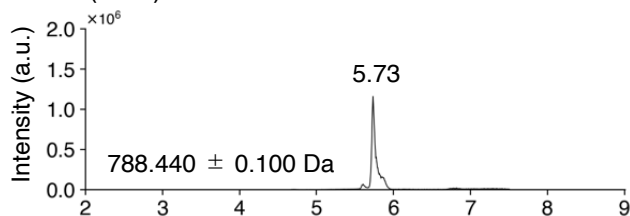
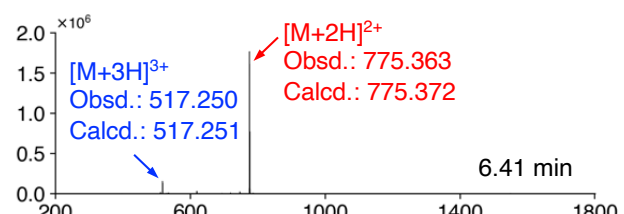
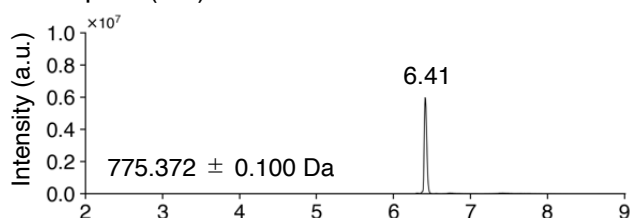
Supplementary Fig. 5: Binding kinetics of macrocyclic peptides against M^{Pro}. SPR sensorgrams of selected peptides and variants. The sequences and kinetic values are shown in Table 1. Five different concentrations (nM), indicated by the numbers above the sensorgrams, of each peptide were injected for measuring kinetic constants. Binding sensorgrams were fitted using the standard 1:1 binding model. Red and black lines indicate raw sensorgrams and fitted curves, respectively.



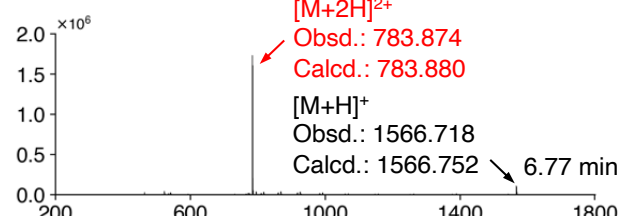
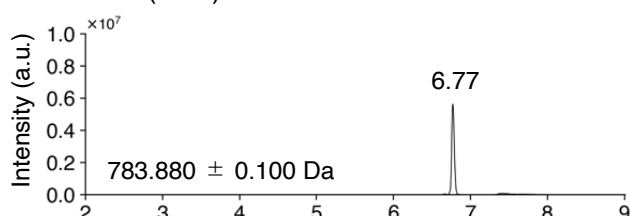
Supplementary Fig. 6: Serum stability assay of macrocyclic peptides. **a**, Structure of the internal standard peptide used in serum stability assays. **b,c**, Chromatogram and mass spectra of reaction mixture after incubation for 24 h (GM1, GM1 γ^1 4A, GM4, GM4H3Q, GM5, and GM5 γ^2 4A) or 1 h (GM2, GM3, GM3 γ^2 10A, and GM4 γ^1 4A). Red and blue arrows indicate $[M+2H]^{2+}$ and $[M+3H]^{3+}$ ions, respectively. Calcd. and Obsd. stand for calculated and observed m/z values of peptides. **d,e**, Chromatogram and mass spectra of fragments GM4-f1–6 and GM4 γ^1 4A-f1–3, respectively. Red and black arrows indicate the $[M+2H]^{2+}$ and $[M+H]^+$ ions, respectively.

C

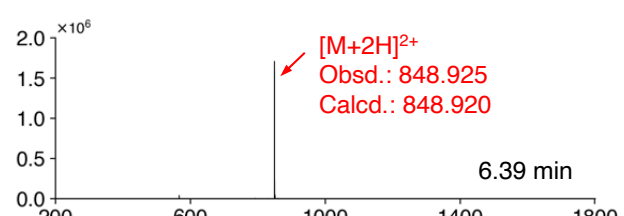
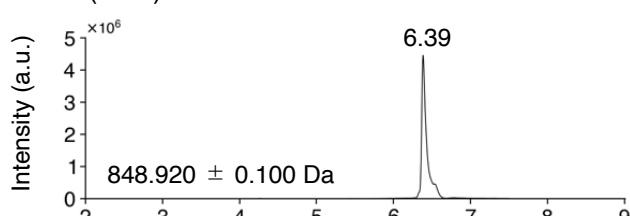
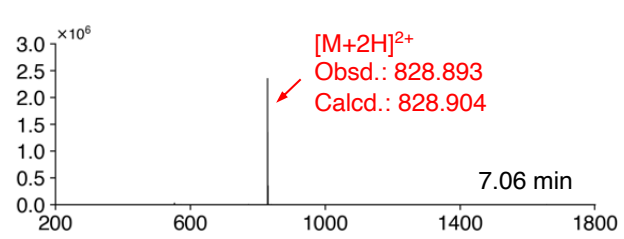
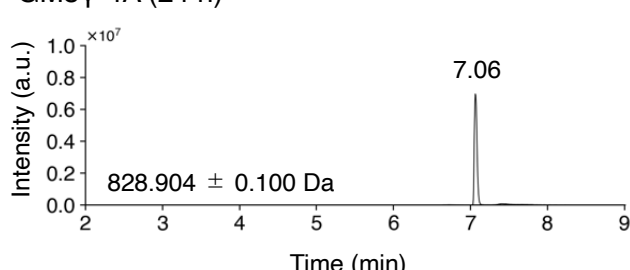
GM4 (24 h)

GM4 γ 4A (1 h)

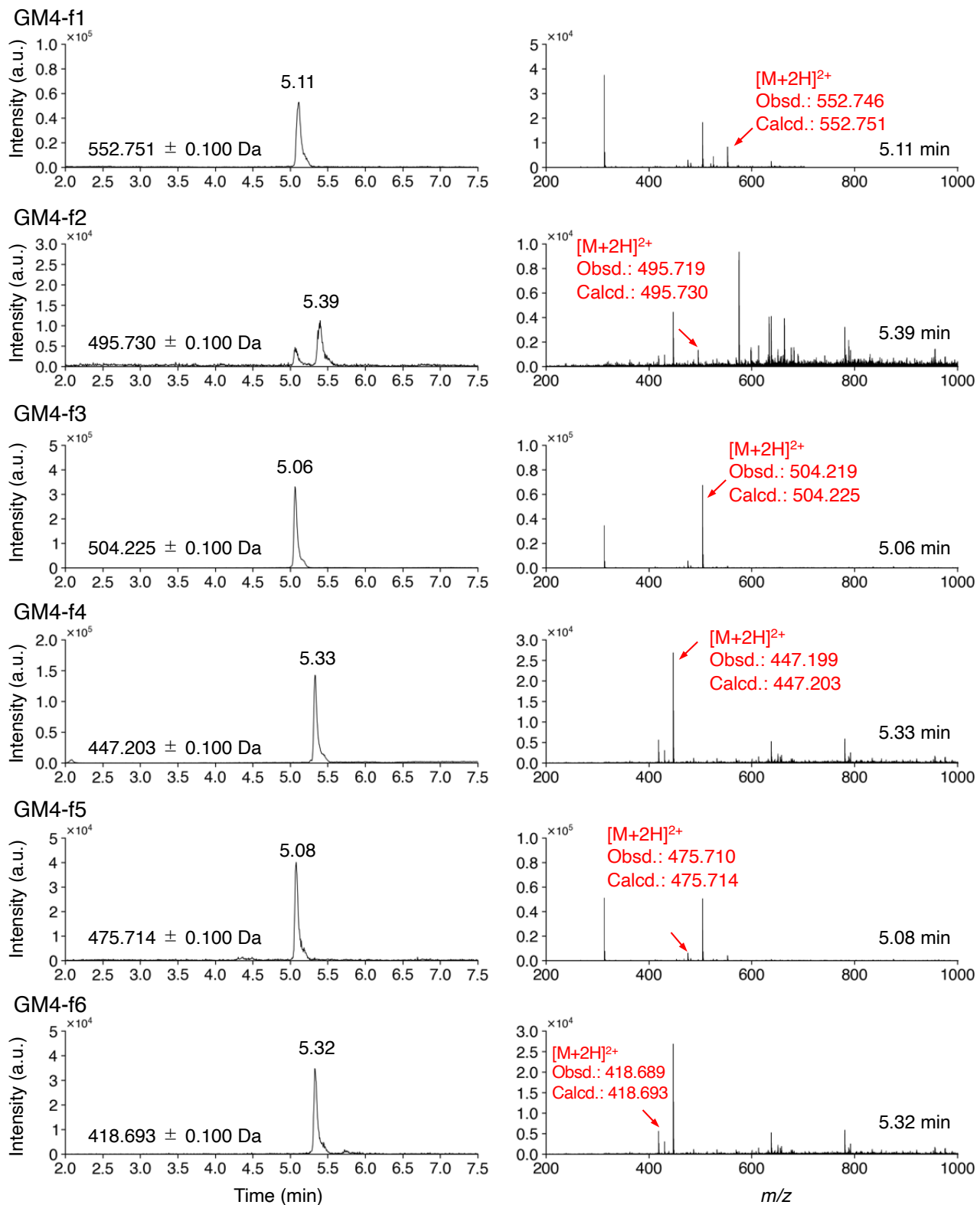
GM4H3Q (24 h)



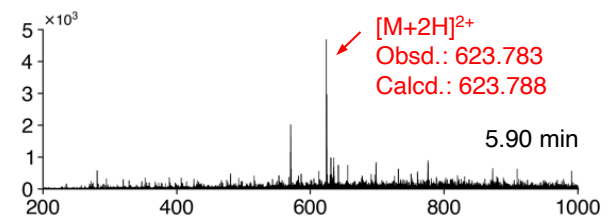
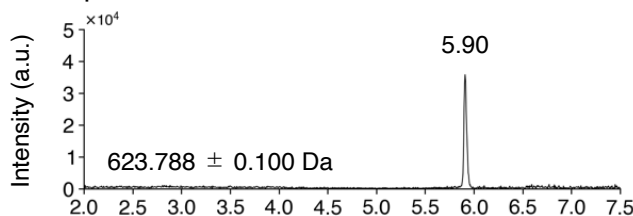
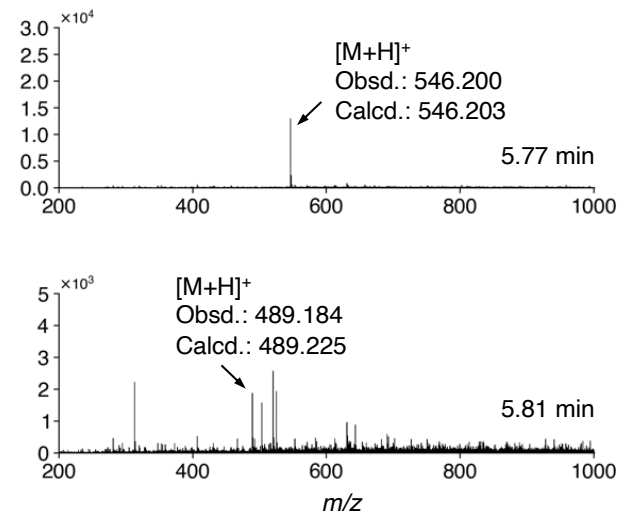
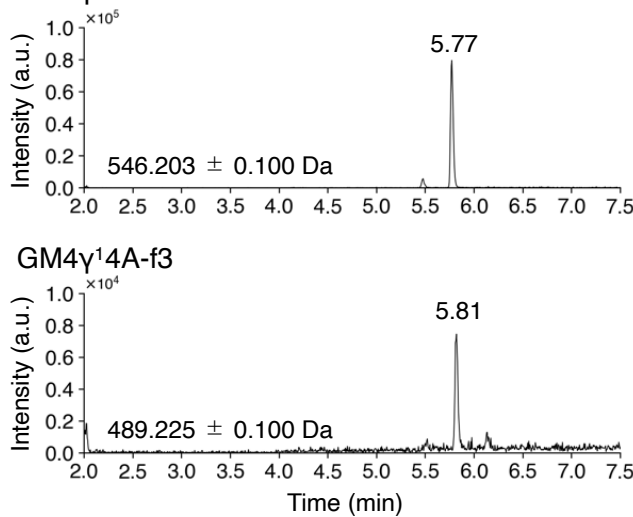
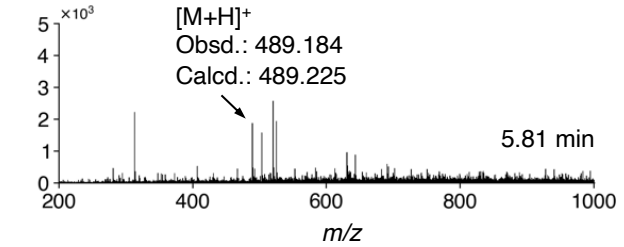
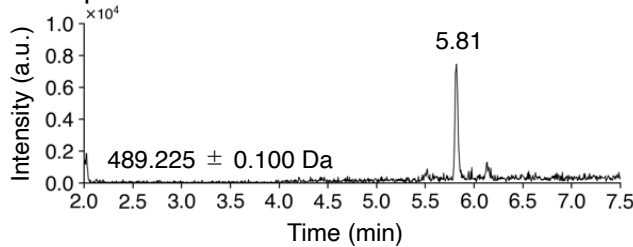
GM5 (24 h)

GM5 γ 4A (24 h)

Supplementary Fig. 6, continued.

d

Supplementary Fig. 6, continued.

eGM4 γ^{14} A-f1GM4 γ^{14} A-f2GM4 γ^{14} A-f3

Supplementary Fig. 6, continued.